Available online at www.sciencedirect.com

ScienceDirect

Journal of the European Ceramic Society 30 (2010) 2117–2122

www.elsevier.com/locate/jeurceramsoc

Inhibition of grain growth in liquid-phase sintered SiC ceramics by AlN additive and spark plasma sintering

Mikinori Hotta *, Junichi Hojo

Department of Applied Chemistry, Faculty of Engineering, Kyushu University, Fukuoka 819-0395, Japan

Received 5 October 2009; received in revised form 3 March 2010; accepted 2 April 2010
Available online 1 May 2010

Abstract

SiC ceramics were prepared from nanosized β-SiC powder with different compositions of AlN and Y_2O_3 sintering additives by spark plasma sintering (SPS) at 1900 °C for 600 s in N_2. The relative density of the sintered SiC specimens increased with increasing amount of AlN, reaching a relative density higher than 99%, while at the same time grain size decreased significantly. The smallest average grain size of 150 nm was observed for SiC sample sintered with 10 vol% of additives consisting of 90 mol% AlN and 10 mol% Y_2O_3. Fully dense nanostructured SiC ceramics with inhibited grain growth were obtained by the AlN additive and SPS technique. The flexural strength of the SiC body containing 70 mol% AlN and 30 mol% Y_2O_3 additives reached the maximum value of 1000 MPa. The SiC bodies prepared with AlN and Y_2O_3 additives had the fracture toughness of around 2.5 $\text{MPam}^{1/2}$.

Keywords: SiC; Sintering; Grain size; Grain growth; Nitrides

1. Introduction

Silicon carbide (SiC) ceramics have been used for structural applications at high temperature because of relatively low density, high hardness, excellent mechanical strength and good thermal stability. However, SiC possesses a strongly covalent bonding. Hence, it is very difficult to densify SiC powder without sintering additives. The conventional densification of SiC is achieved by solid-phase sintering with B and C additives,[1] or liquid-phase sintering with metal oxides additives such as Al_2O_3 and Y_2O_3.[2,3] The mechanical properties of ceramics are largely dependent on the microstructure. The liquid-phase sintered SiC ceramics have high fracture toughness compared with the solid-phase sintered SiC, because the elongated grains can form during liquid-phase sintering.[4,5] Besides, since homogeneous and fine-grained microstructures can be obtained by liquid-phase sintering due to the lower sintering temperatures and the presence of the liquid phase, the excellent mechanical strength for structural applications may be expected in the liquid-phase sintered SiC.[4] The oxide additives react with SiO_2 derived from the surface oxide of SiC particle to form a liquid during sintering process, and the liquid promotes the densification and microstructural development. Meanwhile, amorphous phase is generally present in the grain boundary of the liquid-phase sintered SiC after the sintering owing to the formation of the liquid.[6,7] The residual intergranular amorphous phase significantly affects the high-temperature mechanical properties of the SiC ceramics.[8] In liquid-phase sintered SiC ceramics with AlN and rare-earth oxides additives, remarkable improvements of both high-temperature strength and oxidation resistance have been reported.[8–12] Some researchers have revealed that the advancements were due to the decrease in the residual glassy phase at grain boundary by the formation of SiC–AlN solid solution and to the increase in the heat resistance of the grain boundary by the addition of AlN and rare-earth oxide additives.[13,14]

Spark plasma sintering (SPS) technique allows specimen to heat rapidly because the pulsed direct current used in the technique can pass through the die and punch rods made of graphite.[15] Consequently, the grain growth can be retarded by a shorter time of sintering process. Moreover, low-sinterable

---

* Corresponding author. Present address: Advanced Manufacturing Research Institute, National Institute of Advanced Industrial Science and Technology (AIST), 2266-98 Shimo-Shidami, Moriyama-ku, Nagoya 463-8560, Japan. Tel.: +81 52 736 7120; fax: +81 52 736 7405.

E-mail address: mikinori-hotta@aist.go.jp (M. Hotta).

0955-2219/$ – see front matter © 2010 Elsevier Ltd. All rights reserved.
doi:10.1016/j.jeurceramsoc.2010.04.006

materials can be densified easily at a moderate temperature due to the inhibition of grain growth. The SPS technique is often called by other name such as pulse electric current sintering (PECS),[16–18] field-assisted sintering technique (FAST)[19] and plasma-assisted sintering (PAS),[20] because the generations of spark discharge and/or plasma during SPS process have not been verified. The low-sinterable materials such as Al_2O_3, Si_3N_4, TiN, SiC, SiAlON and composites have been produced as fully dense materials by SPS technique.[16–27]

In our previous study,[25] on SPS of submicron-sized β-SiC powder with AlN and Y_2O_3 additives, the addition of AlN was found to result in a retardation of grain growth during SPS and an increase in mechanical strength for the SiC bodies. Also, when nanosized β-SiC powder containing about 4 mass% of free carbon was sintered with AlN and Y_2O_3 additives by SPS at temperatures of 1800–2000 °C for 600 s, the full densification was not achieved, in which the relative density was 90–95% and the many residual pores were observed in the SiC bodies.[27] This may be attributed to the decrease in the amount of a liquid phase due to reduction of surface oxide of SiC particles by the free carbon in the SiC starting powder.

In the present work, the free carbon in the nanosized β-SiC powder was removed, and dense and fine-grained SiC ceramics were prepared using the resultant β-SiC powder with AlN and Y_2O_3 additives by SPS through the liquid-phase sintering. The effect of AlN additive on densification of the nanosized β-SiC powder and on crystalline phase, microstructure and mechanical properties of the SiC ceramics was investigated.

2. Experimental procedure

Ultra-fine β-SiC powder (Sumitomo Osaka Cement Co., Ltd., Tokyo, Japan, free carbon content: 3.8 mass%, oxygen content: 0.9 mass%) was heated at 700 °C for 2 h in air to remove the free carbon. The powder was treated with HF aqueous solution for 4 h at room temperature to eliminate the surface oxide of the SiC particles formed during the heat treatment. The powder was filtrated and washed with pure water, and then the obtained powder was dried. The content of free carbon of the resultant powder reduced to less than 0.1 mass% and oxygen content was 1.3 mass%. SEM micrograph of the resulting β-SiC powder used as starting material in this study was shown in Fig. 1. The average size of the particles was 40 nm (number mean diameter via SEM image in Fig. 1). AlN (Dow Chemical Co., Midland, Michigan, USA, oxygen content: 2.0 mass%, average particle size: 1.1 μm) and Y_2O_3 (Shin-Etsu Chemical Co., Ltd., Tokyo, Japan, 0.3 μm) powders were added to SiC as sintering additive. The total amount of the additives was fixed at 10 vol%, and the content of AlN additive was varied from 0 to 100 mol%. The additive composition was listed in Table 1. As a reference, 2 mass% Al_2O_3 (Sumitomo chemical Co., Ltd., Tokyo, Japan, α-phase, average particle size: 0.5 μm) was also used as sintering additive. These powders were mixed with a small amount of ethanol. The mixed slurry was dried and then passed through a sieve with a pore-opening size of 300 μm. The mixtures were embedded in a graphite die, and then sintered at a temperature of 1900 °C for a holding time of 600 s under a uniaxial pressure of 30 MPa at a heating rate of 1.7 °C/s by SPS (SPS-515S, SPS SYNTEX INC., Kanagawa, Japan). The mixtures of SiC–AlN–Y_2O_3 and SiC–Al_2O_3 systems were sintered in N_2 and Ar atmospheres, respectively. The temperature on the surface of the die was measured with an optical pyrometer. Linear shrinkage of the powder compacts during the SPS process was continuously monitored by displacement of the punch rod. The densities of the sintered samples were measured by the Archimedes method. The crystalline phase was identified using X-ray diffractometry (XRD; Miniflex, Rigaku Co., Tokyo, Japan) with Cu Kα radiation. The samples were polished with 3 μm diamond slurry and then etched by plasma in CF_4 and O_2 gases. The surfaces of the polished samples were observed by scanning electron microscopy (SEM; S-5200, JEOL Ltd., Tokyo, Japan). The average grain size (number mean diameter) of the SiC bodies was determined from linear intercept length of 100 grains in the SEM pictures of the etched surfaces. Flexural strength was measured by a three-point bending method (Autograph AG-10TC, Shimadzu Co., Kyoto, Japan) on sample size of 2 mm × 2 mm × 15 mm at room temperature.

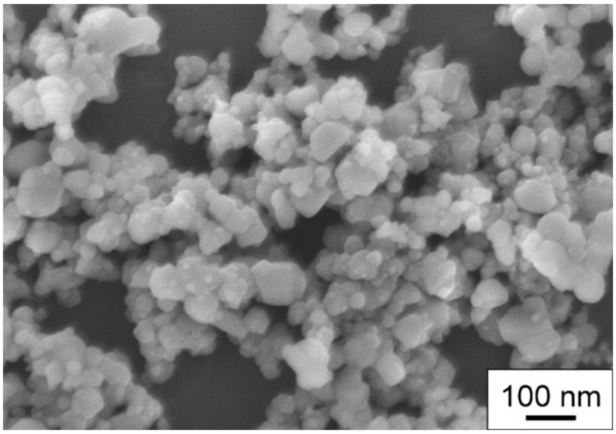

Fig. 1. SEM micrograph of β-SiC starting powder after removing free carbon.

Fracture toughness (K_{IC}) at room temperature was evaluated by a hardness tester (AVK-C2, Akashi Co.) at indentation load (P) of 98 N. The fracture toughness was calculated by Eq. (1) using the half length of the crack (c) formed around the corners of indentations[28]:

$$K_{IC} = 0.073 \times (P/c^{1.5}) \quad (1)$$

Table 1
Average grain size of the SiC bodies sintered with different compositions of AlN–Y_2O_3 additives and with Al_2O_3 additive at 1900 °C for 600 s by SPS.

Sample designation	Additive composition (mol%)		Average grain size (nm)
	AlN	Y_2O_3	
0AN	0	100	1450
10AN	10	90	1120
30AN	30	70	780
50AN	50	50	430
70AN	70	30	320
90AN	90	10	150
100AN	100	0	–
2AO	2 mass% Al_2O_3		1030

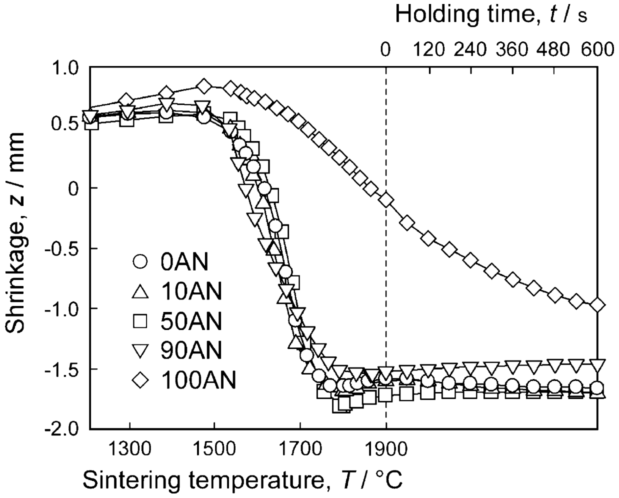

Fig. 2. Effect of sintering temperature on the displacement of the powder compacts containing different compositions of AlN–Y_2O_3 additives up to 1900 °C, and the time dependence of isothermal displacement at 1900 °C up to 600 s during SPS process.

3. Results and discussion

Fig. 2 shows the displacement of the powder compacts containing different amounts of AlN additive with elevating temperature up to 1900 °C during SPS process. The isothermal displacement at 1900 °C up to 600 s is also shown in Fig. 2. The shrinkage of the compacts started at 1450–1500 °C. The compact containing 90 mol% AlN additive had the highest shrinkage rate at the initial stage of shrinkage. The shrinkage of the compacts containing 0–90 mol% AlN additive ceased at 1780–1800 °C. The compact containing 100 mol% AlN additive continued to shrink during holding at 1900 °C. In our previous study,[25] using submicron-sized β-SiC powder, the beginning temperature of shrinkage for the compacts containing 10–90 mol% AlN was about 1480 °C, indicating almost the same as that for the compacts using nanosized β-SiC powder. Furthermore, the shrinkage of the compact containing 90 mol% AlN finished during holding time of 600 s at 1900 °C. This suggested that the finishing temperature of the shrinkage for nanosized β-SiC powder was lower over 100 °C than that for submicron-sized β-SiC.

Fig. 3 presents the relative density of the SiC bodies prepared with different compositions of AlN and Y_2O_3 additives at 1900 °C for 600 s. The density of the sample without AlN additive was 96%. For the samples containing 10–90 mol% AlN additive, the density increased with increasing AlN content, and that of the sample containing 90 mol% AlN additive reached more than 99%. The density of specimens prepared from submicron-sized β-SiC powder also increased with increasing content of AlN additive.[25] The density of the sample containing 100 mol% AlN additive decreased to 88%. These densities were higher than those of the SiC specimens prepared from nanosized β-SiC powder containing 4 mass% free carbon at sintering temperatures of 1800–2000 °C for 600 s by SPS.[27] In the samples sintered with 2 mass% Al_2O_3 additive, the high density of 99% was achieved.

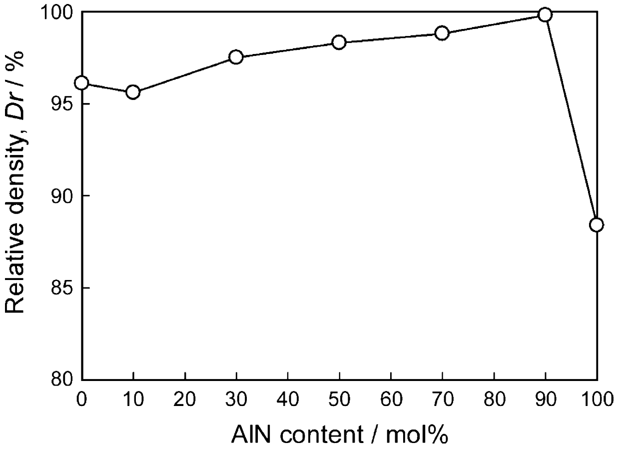

Fig. 3. Effect of the amount of AlN additive on the relative density of the SiC bodies sintered at 1900 °C for 600 s by SPS.

The densification was promoted by the addition of 90 mol% AlN to SiC–Y_2O_3 system, as evidenced by the higher relative density in Fig. 3. It is known that the eutectic temperature of a SiO_2–Y_2O_3 system is 1660 °C.[29] When Al_2O_3 is added to the SiO_2–Y_2O_3 system, the eutectic temperature decreases to less than 1400 °C, as is evident from the phase diagram of a SiO_2–Al_2O_3–Y_2O_3 system.[30] In the present work, the SiO_2–Al_2O_3–Y_2O_3 liquid phase derived from the surface oxides of SiC and AlN particles may be formed, because the eutectic temperature of the SiO_2–Al_2O_3–Y_2O_3 system is lower than sintering temperature. Therefore, the densification of the SiC compacts containing AlN and Y_2O_3 additives might be due to the liquid-phase sintering. In fact, the starting temperature of the shrinkage, 1450–1500 °C, was almost the same as the eutectic temperature. A large amount of the liquid phase might form with

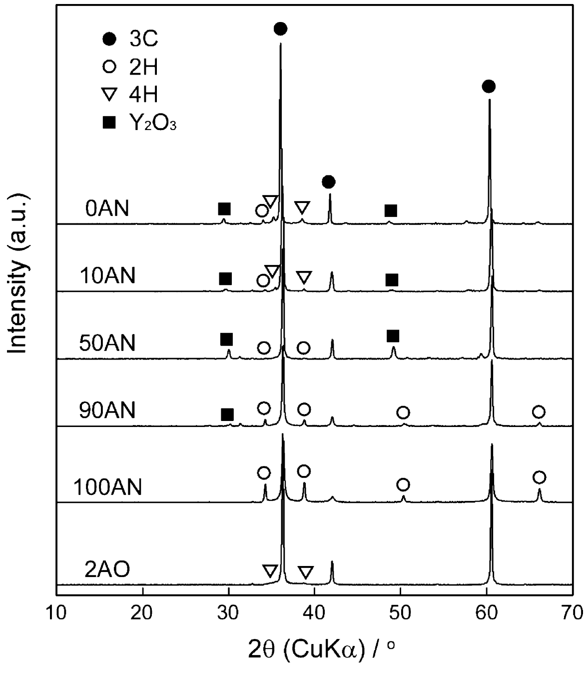

Fig. 4. XRD patterns of the SiC bodies sintered with different compositions of AlN–Y_2O_3 additives and with Al_2O_3 additive at 1900 °C for 600 s by SPS.

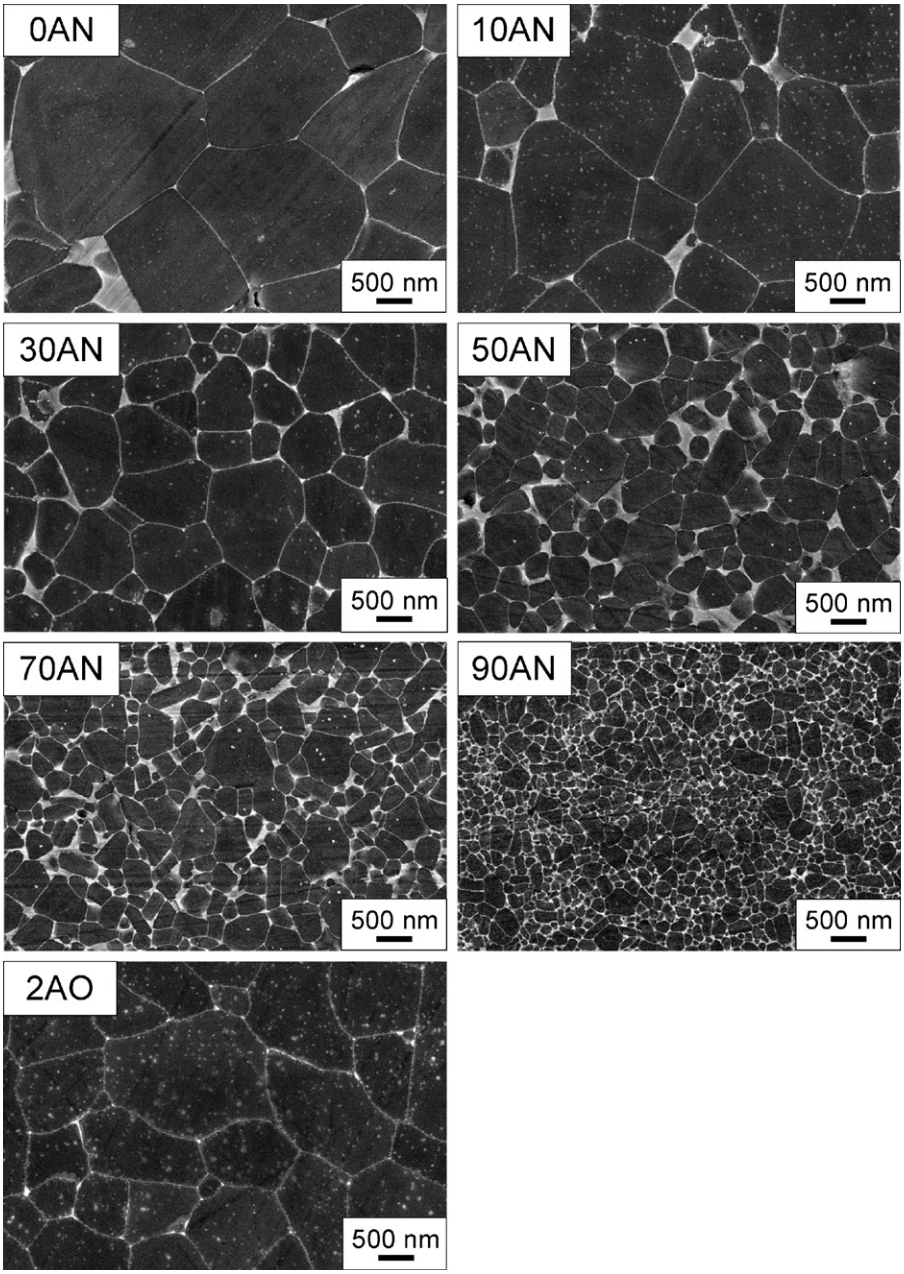

Fig. 5. SEM micrographs of the etched surface of the SiC bodies sintered with different compositions of AlN–Y_2O_3 additives and with Al_2O_3 additive at 1900 °C for 600 s by SPS.

increasing AlN content, that is, an increase in Al_2O_3 amount derived from the surface oxide of AlN, leading to acceleration of the densification. It is known that the eutectic temperature of AlN–Y_2O_3 system is about 1830 °C.[31,32] As the finishing temperature of the shrinkage around 1800 °C was lower than the eutectic temperature (Fig. 2), the AlN–Y_2O_3 liquid phase would not contribute to the densification.

Fig. 4 shows the XRD patterns of the SiC bodies prepared with different compositions of AlN and Y_2O_3 additives and with 2 mass% Al_2O_3 additive at 1900 °C for 600 s. When Y_2O_3 only was added to SiC, the XRD peak of Y_2O_3 was detected after sintering. The peak of Y_2O_3 decreased by the addition of AlN, even at a small amount of AlN additive. This tendency was identical to the result in the sintering of submicron-sized β-SiC powder with AlN and Y_2O_3 additives by SPS.[25] The crystalline phase appearing in the samples was mainly 3C (β-SiC). The peaks of 2H and 4H (α-SiC) phases were detected in the sample without AlN additive. When the amount of AlN additive increased from 10 to 90 mol%, the peak of 4H phase disappeared and the peak intensity of 2H phase increased. In the specimen prepared using Al_2O_3 additive, 4H phase was identified. Hence, the use of AlN additive for sintering of 3C-SiC powder inhibits the phase transformation from 3C- to 4H-SiC and enhances the transformation to 2H-SiC. AlN is possible to form a solid solution with 2H-SiC, because AlN has 2H structure and is soluble in 2H-SiC.[33] In our previous study on SiC–AlN composite, the dissolution of

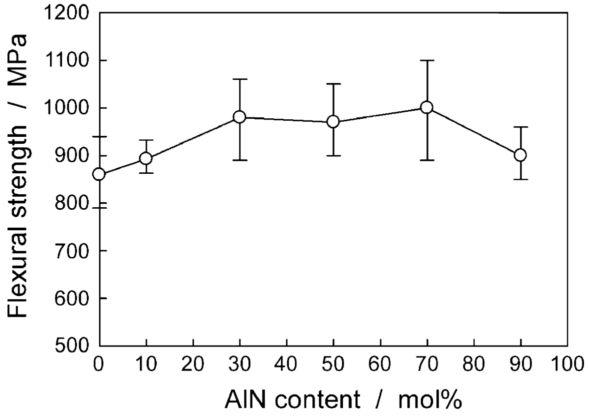

Fig. 6. Effect of the amount of AlN additive on the flexural strength of the SiC bodies sintered at 1900 °C for 600 s by SPS.

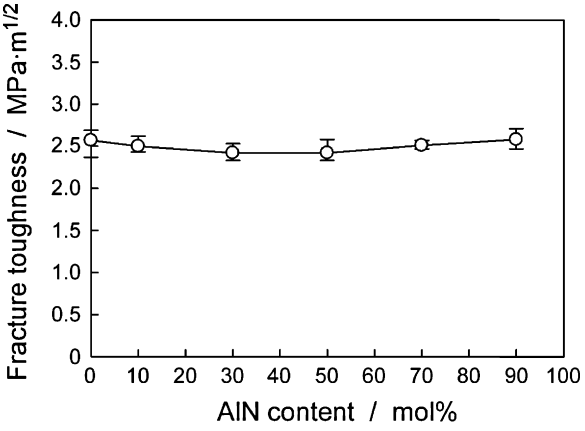

Fig. 7. Effect of the amount of AlN additive on the fracture toughness of the SiC bodies sintered at 1900 °C for 600 s by SPS.

AlN to SiC promoted the phase transformation from 3C- to 2H-SiC.[34,35] Therefore, 2H phase in the SiC bodies sintered using AlN additive suggested the existence of AlN and/or SiC–AlN solid solution.

Fig. 5 shows the SEM micrographs of the etched surface of the SiC bodies prepared with different compositions of AlN and Y_2O_3 additives and with 2 mass% Al_2O_3 additive at 1900 °C for 600 s. Table 1 summaries the average grain size of the SiC bodies determined from the SEM images. The grain size of the samples sintered with 10–90 mol% AlN additive was smaller than that of the sample sintered without AlN additive. When the amount of AlN additive increased, the grain size decreased. This result was similar to SiC ceramics fabricated using submicron-sized β-SiC powder with AlN and Y_2O_3 additives.[25] The grain size for the fully dense sample prepared using 90 mol% AlN additive was 150 nm. In the specimen prepared with Al_2O_3 additive, on the other hand, the grain grew to the size of about 1 μm, and the grain size was larger than those of the samples prepared with 30–90 mol% AlN additive. Therefore, the use of AlN additive inhibited the growth of nanosized SiC grains, although the SiC grains grew from 40 nm in the starting powder to 150 nm in the sintered body. Increase in the amount of AlN additive would lead to an increase in the viscosity of a liquid formed from SiC–AlN–Y_2O_3 system at 1900 °C.[36] Hence, the inhibition of the grain growth by increasing amount of AlN additive might be due to the increase in the viscosity by the formation of a nitrogen-containing liquid, although a large amount of the liquid generally facilitates the grain growth through solution-reprecipitation. Moreover, the inclusion of AlN in 2H-SiC grains might lead to the suppression of mass transfer in SiC grains. In contrast, when AlN remains as secondary phase without including in 2H-SiC grains, the growth of SiC grains might be inhibited by pinning effect.

Fig. 6 demonstrates the flexural strength of the SiC bodies prepared with different compositions of AlN and Y_2O_3 additives at 1900 °C for 600 s. The flexural strength increased with an increase in AlN content. This might be due to the increase in the density and the decrease in the grain size of the samples. The sample containing 70 mol% AlN additive had the maximum strength of 1000 MPa. The strength of the sample containing 90 mol% AlN additive was lower than that of the sample containing 70 mol% AlN additive, although the grain size decreased with increasing AlN content as shown in Table 1. The strength of the dense SiC body prepared with 2 mass% Al_2O_3 additive was 900 MPa. These results mean that the fracture strength depends on not only the grain size of microstructure but also the composition of grain boundary phase.

Fig. 7 shows the fracture toughness of the SiC bodies prepared with different compositions of AlN and Y_2O_3 additives at 1900 °C for 600 s. The fracture toughness of the SiC bodies was 2.4–2.6 MPam$^{1/2}$, almost independent of AlN content. The low toughness would be due to the equiaxed grain structure in the SiC bodies (Fig. 5). The SiC body prepared with Al_2O_3 additive had the fracture toughness of 2.7 MPam$^{1/2}$, indicating almost the same as the toughness of SiC bodies prepared with AlN and Y_2O_3 additives.

4. Conclusions

Using nanosized β-SiC starting powder with the particle size of 40 nm, SiC ceramics were prepared with 10 vol% of total amount of sintering additive, consisting of different compositions of AlN and Y_2O_3, at a temperature of 1900 °C for 600 s in N_2 by SPS. Densification, phase transformation and microstructure of the SiC sintered bodies were studied. The shrinkage of the powder compacts started at 1450–1500 °C and finished at 1780–1800 °C. With increasing amount of AlN additive, the relative density of the specimens increased and the size of the SiC grains decreased. The phase transformation from 3C- to 4H-SiC was inhibited and the transformation to 2H-SiC was accelerated with an increase in the AlN additive. Dense SiC body prepared at composition of 90 mol% AlN and 10 mol% Y_2O_3 additives had the smallest grain size of 150 nm. The flexural strength of the fine-grained SiC body was 900 MPa. On the other hand, the strength of the SiC body containing 70 mol% AlN and 30 mol% Y_2O_3 additives reached the maximum value of 1000 MPa. The fracture toughness of the SiC bodies prepared with AlN and Y_2O_3 additives was 2.4–2.6 MPam$^{1/2}$.

Acknowledgment

This work was performed as Research Fellow of the Japan Society for the Promotion of Science (No. 07570).

References

1. Prochazka S. The role of boron and carbon in the sintering of silicon carbide. In: Popper P, editor. *Special ceramics 6*. Stoke-on-Trent, UK: British Ceramic Research Association; 1975. p. 171–81.
2. Omori M, Takei H. Pressureless sintering of SiC. *J Am Ceram Soc* 1982;**65**. C-92.
3. Mulla MA, Krstic VD. Low-temperature pressureless sintering of β-silicon carbide with aluminum oxide and yttrium oxide additions. *Am Ceram Soc Bull* 1991;**70**:439–43.
4. Padture NP. In situ-toughened silicon carbide. *J Am Ceram Soc* 1994;**77**:519–23.
5. Kim Y-W, Mitomo M, Hirotsuru H. Grain growth and fracture toughness of fine-grained silicon carbide ceramics. *J Am Ceram Soc* 1995;**78**:3145–8.
6. Padture NP, Lawn BR. Toughness properties of a silicon carbide with an in situ induced heterogeneous grain structure. *J Am Ceram Soc* 1994;**77**:2518–22.
7. Mitomo M, Kim Y-W, Hirotsuru H. Fabrication of silicon carbide nanoceramics. *J Mater Res* 1996;**11**:1601–4.
8. Keppeler M, Reichert H-G, Broadley JM, Thurn G, Wiedmann I, Aldinger F. High temperature mechanical behaviour of liquid phase sintered silicon carbide. *J Eur Ceram Soc* 1998;**18**:521–6.
9. Rixecker G, Wiedmann I, Rosinus A, Aldinger F. High-temperature effects in the fracture mechanical behaviour of silicon carbide liquid-phase sintered with AlN-Y_2O_3 additives. *J Eur Ceram Soc* 2001;**21**:1013–9.
10. Kim Y-W, Mitomo M, Nishimura T. High-temperature strength of liquid-phase-sintered SiC with AlN and Re_2O_3 (RE = Y, Yb). *J Am Ceram Soc* 2002;**85**:1007–9.
11. Choi H-J, Lee J-G, Kim Y-W. Oxidation behavior of liquid-phase sintered silicon carbide with aluminum nitride and rare-earth oxides. *J Am Ceram Soc* 2002;**85**:2281–6.
12. Strecker K, Hoffmann M-J. Effect of AlN-content on the microstructure and fracture toughness of hot-pressed and heat-treated LPS-SiC ceramics. *J Eur Ceram Soc* 2005;**25**:801–7.
13. Kim Y-W, Mitomo M, Nishimura T. Heat-resistant silicon carbide with aluminum nitride and erbium oxide. *J Am Ceram Soc* 2001;**84**:2060–4.
14. Suzuki K, Sasaki M. Microstructure and mechanical properties of liquid-phase-sintered SiC with AlN and Y_2O_3 additions. *Ceram Int* 2005;**31**:749–55.
15. Tokita M. Trends in advanced SPS spark plasma sintering system and technology. *J Soc Powder Technol Jpn* 1993;**30**:790–804.
16. Zhou Y, Hirao K, Toriyama M, Tanaka H. Very rapid densification of nanometer silicon carbide powder by pulse electric current sintering. *J Am Ceram Soc* 2000;**83**:654–6.
17. Suganuma M, Kitagawa Y, Wada S, Murayama N. Pulsed electric current sintering of silicon nitride. *J Am Ceram Soc* 2003;**86**:387–94.
18. Zhou Y, Hirao K, Yamauchi Y, Kanzaki S. Densification and grain growth in pulse electric current sintering of alumina. *J Eur Ceram Soc* 2004;**24**:3465–70.
19. Groza JR, Curtis JD, Krämer M. Field-assisted sintering of nanocrystalline titanium nitride. *J Am Ceram Soc* 2000;**83**:1281–3.
20. Schneider JA, Risbud SH, Mukherjee AK. Rapid consolidation processing of silicon nitride powders. *J Mater Res* 1996;**11**:358–62.
21. Nishimura T, Mitomo M, Hirotsuru H, Kawahara M. Fabrication of silicon nitride nano-ceramics by spark plasma sintering. *J Mater Sci Lett* 1995;**14**:1046–7.
22. Shen Z, Johnsson M, Zhao Z, Nygren M. Spark plasma sintering of alumina. *J Am Ceram Soc* 2002;**85**:1921–7.
23. Tatami J, Iguchi M, Hotta M, Zhang C, Komeya K, Meguro T, et al. Fabrication and evaluation of Ca-α SiAlON nano ceramics. *Key Eng Mater* 2003;**237**:105–10.
24. Hotta M, Goto T. Densification and microstructure of Al_2O_3-cBN composites prepared by spark plasma sintering. *J Ceram Soc Jpn* 2008;**116**:744–8.
25. Hotta M, Hojo J. Effect of AlN additive on densification, microstructure and strength of liquid-phase sintered SiC ceramics by spark plasma sintering. *J Ceram Soc Jpn* 2009;**117**:1009–12.
26. Hotta M, Hojo J. Nanostructure control of liquid-phase sintered Si_3N_4 ceramics by spark plasma sintering. *J Ceram Soc Jpn* 2009;**117**:1302–5.
27. Hotta M, Enomoto N, Hojo J. Liquid-phase sintered silicon carbide with aluminum nitride and rare-earth oxide additives. *Key Eng Mater* 2006;**317–318**:111–4.
28. Lawn BR, Fuller ER. Equilibrium penny-like cracks in indentation fracture. *J Mater Sci* 1975;**10**:2016–24.
29. Levin EM, Robbins CR, McMurdie HF. In: Reser MK, editor. *Fig. 2388 in phase diagrams for ceramists*. Columbus, OH: American Ceramic Society; 1964.
30. Levin EM, Robbins CR, McMurdie HF. In: Reser MK, editor. *Fig. 2586 in phase diagrams for ceramists*. Columbus, OH: American Ceramic Society; 1964.
31. Jeutter A. *Untersuchung der Phasenbeziung im System Aluminiumnitrid-Yttriumoxid*. Diplomarbeit an Universitat Stuttgart; 1993.
32. Izhevskyi VA, Genova LA, Bressiani AHA, Bressiani JC. Microstructure and properties tailoring of liquid-phase sintered SiC. *Int J Refract Met Hard Mater* 2001;**19**:409–17.
33. Zangvil A, Ruh R. Phase relationships in the silicon carbide–aluminum nitride system. *J Am Ceram Soc* 1988;**71**:884–90.
34. Shirouzu K, Nonaka Y, Hotta M, Enomoto N, Hojo J. Synthesis and microstructural evaluation of SiC-AlN composites. *Key Eng Mater* 2007;**352**:193–6.
35. Shirouzu K, Ohkusa T, Kawamoto T, Enomoto N, Hojo J. Evaluation on microstructure and dissolution behavior of SiC-AlN composites prepared by SPS process. *J Ceram Soc Jpn* 2008;**116**:781–5.
36. Kim Y-W, Mitomo M. Fine-grained silicon carbide ceramics with oxynitride glass. *J Am Ceram Soc* 1999;**82**:2731–6.